

Article

Identifying Ecological Security Patterns Based on Ecosystem Service Supply and Demand Using Remote Sensing Products (Case Study: The Fujian Delta Urban Agglomeration, China)

Xiaonan Niu ¹, Huan Ni ^{2,*}, Qun Ma ³, Shangxiao Wang ¹  and Leli Zong ¹¹ Nanjing Center, China Geological Survey, Nanjing 210016, China² School of Remote Sensing & Geomatics Engineering, Nanjing University of Information Science & Technology, Nanjing 210044, China³ School of Environmental and Geographical Sciences, Shanghai Normal University, Shanghai 200234, China

* Correspondence: nih@nuist.edu.cn

Abstract: As the global population increases and cities expand, increasing social needs and ecosystem degradation generally coexist, especially in China's urban agglomerations. Identifying ecological security patterns (ESPs) for urban agglomerations serves as an effective way to sustain regional ecological security and promote harmonious ecological conservation and economic development. Focusing on the Fujian Delta Urban Agglomeration (FDUA) as an example, this study aims to present a framework for linking the supply and demand of ecosystem services (ESs) to identify ESPs in 2020. First, the ecological sources are delimited by coupling the supply and demand of four critical ESs (carbon storage, water provision, grain production, and outdoor recreation). Afterward, the resistance coefficient is modified using nighttime light intensity data and the ecological risk index, the second of which combines the effects of the soil erosion sensitivity index, the geological disaster risk index, and the land desertification risk index. Then, ecological corridors are determined by employing the minimum cumulative resistance method. With the integration of ecological sources and corridors, the ESPs of the FDUA can be identified. The results show a distinct supply–demand mismatch for ESs, with supply exhibiting an upward gradient from coastal cities to inland mountain cities and demand showing the opposite trend. The ESPs consist of 8359 km² of ecological sources that are predominantly forests, 171 ecological corridors with a total length of 789.04 km, 34 pinch points, 26 barriers, and 48 break points. This paper presents a realizable approach for constructing ESPs for urban agglomerations, which will help decision makers optimize ecological sources and ecological protection policies.

Keywords: ecological security pattern; ecosystem services supply and demand; ecological sources; ecological corridor; fujian delta urban agglomeration



check for updates

Citation: Niu, X.; Ni, H.; Ma, Q.; Wang, S.; Zong, L. Identifying Ecological Security Patterns Based on Ecosystem Service Supply and Demand Using Remote Sensing Products (Case Study: The Fujian Delta Urban Agglomeration, China). *Sustainability* **2023**, *15*, 578. <https://doi.org/10.3390/su15010578>

Academic Editor: Jakub Brom

Received: 31 October 2022

Revised: 9 December 2022

Accepted: 17 December 2022

Published: 29 December 2022



Copyright: © 2022 by the authors. Licensee MDPI, Basel, Switzerland. This article is an open access article distributed under the terms and conditions of the Creative Commons Attribution (CC BY) license (<https://creativecommons.org/licenses/by/4.0/>).

1. Introduction

As the global population continues to grow and urban built-up areas expand, urban land transformation will be one of the most irreversible human impacts on the global biosphere [1–3]. The transformation of land use patterns, especially the remarkable loss of ecological land, has changed ecosystem structures and processes and, thus, caused various problems, including landscape fragmentation, biodiversity loss, soil erosion, and water pollution [4–9]. Identifying ways to decrease the negative effect of urbanization on the ecological environment and to achieve urban sustainability has become essential.

An ecological security pattern (ESP) describes an underlying spatial pattern of ecosystems delineated to preserve natural biodiversity and a sustainable supply of ecosystem services (ESs) in a given region [10–12]. The construction of an ESP is an effective way to guarantee urban ecological security. ESPs comprise strategic landscape points and patches

that are vital to the safeguarding and control of certain ecological processes [13]. Current paradigms for constructing ESPs consist of ecological source identification, ecological resistance surface construction, and ecological corridor recognition [14–16].

Specifically, ecological source selection is the first and most basic step in constructing an ESP. Ecological sources are patches that perform important ES functions, which are generally identified by two main approaches. In the first approach, large ecological patches, such as nature reserves, forested land, and habitats, are directly selected as source areas [17,18]. This method ignores the ecosystem conditions of the region, although it is simple and convenient. The second way to determine ecological sources is by constructing evaluation systems in which ecological sensitivity, ES function, ecological adaptability, and ecological risk are usually considered [19,20]. Among these approaches, the most popular view is the assessment of ecological importance in the consideration of ESs [14]. ESs can be viewed as a bridge linking natural systems to human wellbeing [21,22]. ESs are how ecosystems provide products, as well as services such as food supply, water retention, carbon storage, and recreation, to humans [23,24]. The purpose of identifying ecological sources is to find ecological patches with more ESs to satisfy the consumption demands of humans [25]. However, most studies have focused only on the supply of ESs in ecological source identification, with less attention given to the potential to meet the ecological demand of human society. Consequently, it is difficult to provide sufficient information to characterize sustainable ecological patterns without trade-offs between the supply and demand of ESs.

In fact, the concept of ESs was initially developed as a human-centered perspective and intended to improve human well-being and achieve sustainable development. The increasing demand and excessive use of ESs by humans could cause a shortage in the supply of ESs and pose a serious threat to ecosystem security [26,27]. Therefore, incorporating both ES supply and demand in ESP construction can help regulate the tradeoffs between economic growth and ecological protection and enhance the social value of research results [28–30]. Although there has been increasing concern over the past decade about the significance of considering the demand for ESs [31], there are few cases wherein supply–demand analysis has been used for source identification in ESP construction.

The Fujian Delta Urban Agglomeration (FDUA) is an essential node of the West Straits Economic Zone of China and a departure point of the Maritime Silk Road. Increasingly intense urban development has affected local landscape pattern characteristics to a large extent and further brought about many ecological issues, including ES function degradation. At present, the FDU is suffering from an issue related to the association between ecological protection and socioeconomic development. To address this issue, the FDU is selected as the study area of this paper. Specifically, the objectives of the paper are to (1) assess both the supply and demand of ESs by considering water provision, carbon storage, grain production, and outdoor recreation; (2) identify ecological sources by linking supply and demand for ESs; (3) extract ecological corridors by employing the minimum cumulative resistance (MCR) method with the resistance coefficient corrected by nighttime light intensity (NLI) data and the ecological risk index, which is calculated by integrating multiple risk factors, such as the geological disaster risk index, the soil erosion sensitivity index, and the land desertification risk index; and (4) provide advice on the optimization of ecological sources and the development of ecological policies based on the identified ESPs for the FDU.

2. Materials and Methods

2.1. Study Area

Located on the southeastern coast of China, the FDU (116°53′–119°01′ E, 23°33′–25°56′ N) includes the cities of Xiamen, Zhangzhou, and Quanzhou, as shown in Figure 1. The region covers an area of 2.53×10^4 km², accounting for 20.87% of the land area of Fujian Province. The region has complex geomorphological conditions and is a hilly and basin plain area. The inland landscape is mainly composed of low hills. The northern part of the

area is high in altitude, effectively preventing cold air from traveling south and forming the natural green barrier of the FDU. The southern part is mostly composed of a river valley basin and a coastal plain, which is significantly influenced by the subtropical maritime monsoon climate. The overall ecological environment is good, with a forest coverage rate of approximately 61.3%. However, due to the special topographic conditions of narrow coastal zones and limited buffering capacity, ecological security problems, such as damage to key ecological service functions, disturbances of ESPs, and decreasing security space, are particularly prominent. The cities and towns in the region are vulnerable to natural disasters, such as typhoons and floods.

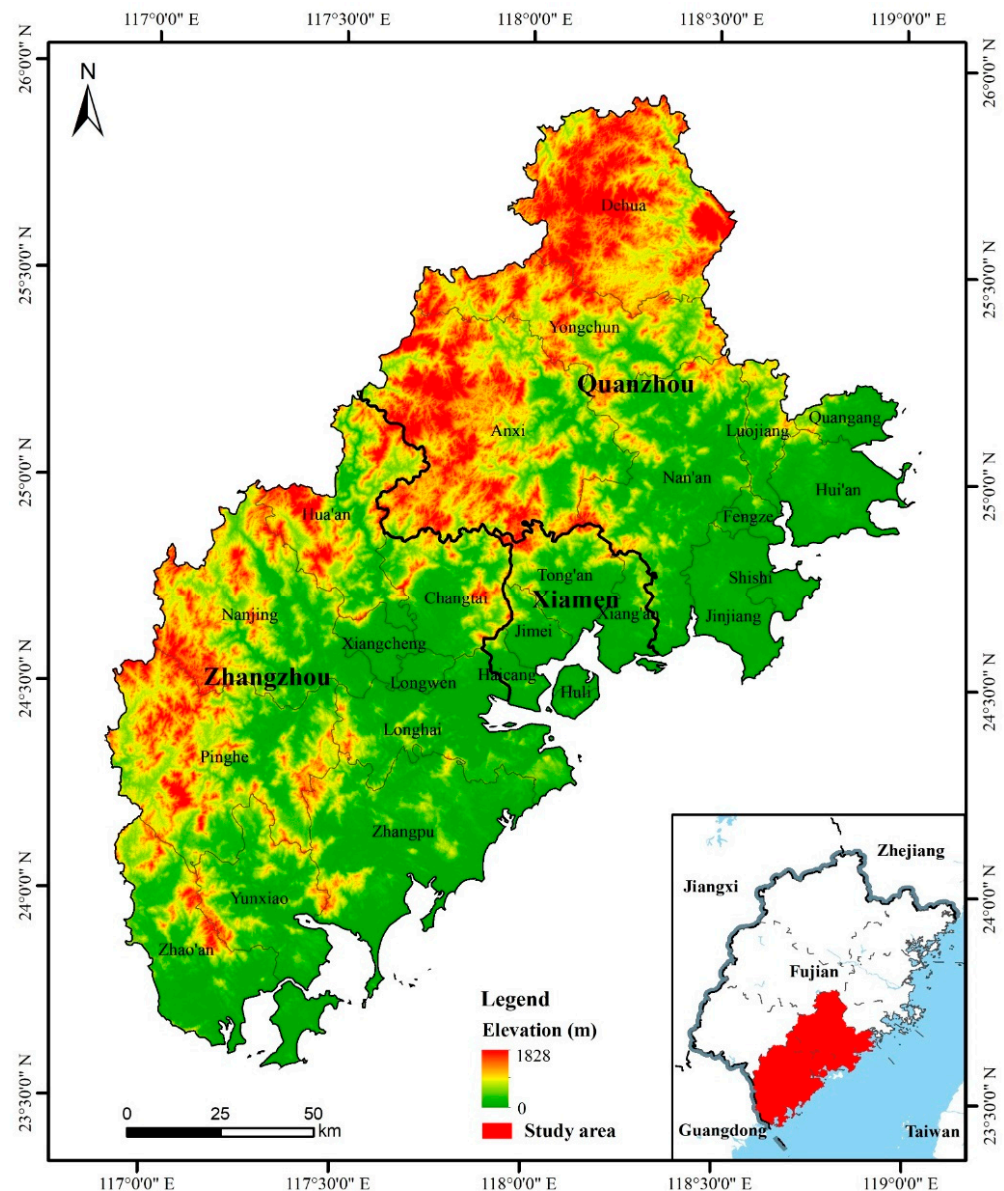


Figure 1. Geographic location of (right) the Fujian Delta Urban Agglomeration and (left) its administrative divisions.

As one of the coastal development areas in China, the FDU has undergone rapid economic development in recent years. According to the Fujian Statistical Yearbook, by the end of 2020, the region's gross domestic product (GDP) was CNY 2108.83 billion, and the total population reached 19.03 million, accounting for 48.03% and 45.73% of the GDP and the population of Fujian Province, respectively. With continuous urbanization and concentration, demand for ESs has grown significantly, resulting in a dramatic decrease

in ecological resources. Human activities have disrupted natural ecological processes and regional ecosystem balance to a certain extent. Because of the great challenges to ecological security and the sustainable development of human society, identifying ESPs by analyzing the imbalance of ES supply and demand has become an urgent issue.

2.2. Data Sources

In this study, the following datasets were used:

1. Land use and land cover (LULC) data for 2020 were derived from the Resource and Environmental Science Data Center (<http://www.resdc.cn/> (accessed on 28 July 2021)).
2. Digital elevation model (DEM) data were provided by the geospatial data cloud (<http://www.gscloud.cn/> (accessed on 10 June 2020)).
3. Normalized Difference Vegetation Index (NDVI) data for 2020 were derived from the MOD13Q1 dataset, with a spatial resolution of 250 m (<http://lpdaac.usgs.gov/> (accessed on 28 July 2021)).
4. Evapotranspiration (ET) data for 2020 were derived from the MOD16A3 dataset, with a spatial resolution of 500 m.
5. Annual precipitation data for 2020 and multiyear average precipitation data were downloaded from the National Earth System Science Data Center, with a spatial resolution of 1 km (<http://www.geodata.cn/> (accessed on 28 July 2021)).
6. Annual runoff data for 2020, with a spatial resolution of 30 m, were provided by China Geographic Scientific Data (www.csdn.store (accessed on 28 July 2021)).
7. Carbon storage data for 2015 were mainly obtained from the China National Ecological Science Data Center (<http://www.cnern.org.cn/> (accessed on 4 August 2021)).
8. Population data, grain yield, and consumption data were obtained from the Statistical Yearbook published by the Fujian Municipal Bureau of Statistics (<http://tjj.fujian.gov.cn/> (accessed on 4 August 2021)). Water consumption data were obtained from the Fujian Bulletin of Water Resources.
9. NPP VIIRS nighttime light data of an annual product for 2020, with a spatial resolution of 15 arc second (approximately 500 m), were provided by the NOAA/NGDC (https://eogdata.mines.edu/nighttime_light/annual/v21/2020/ (accessed on 4 August 2021)).
10. Slope and aspect data were derived from the DEM, lithology data were obtained from geological surveys, and distance-to-river and distance-to-fault data were obtained through ArcGIS software, as necessary parameters for geological disaster risks evaluation.
11. Soil erosion special survey and monitoring data were derived from a comprehensive survey and evaluation of the carrying capacity of resources and the environment in Fujian Province from Nanjing Center, China Geology Survey (Table 1).

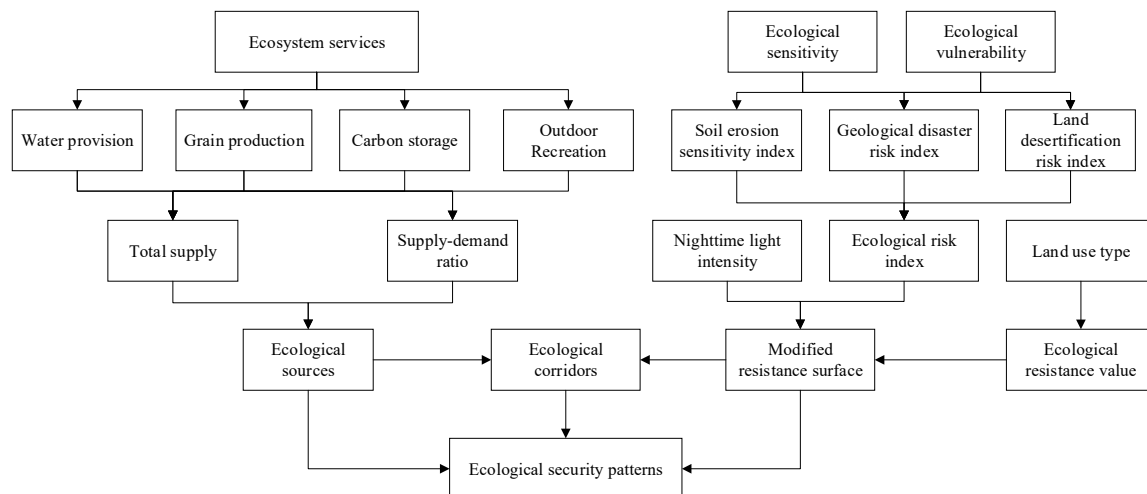
All data were converted to a common spatial reference (CGCS2000/Gauss–Kruger zone 20), and the grid of raster data was resampled to 100 m × 100 m.

2.3. Methods

This study emphasized ecological sources coupling the supply and demand of ESs for the purpose of constructing ESPs. By recognizing and maintaining the crucial spatial pattern, the sustainability of ESs within a given region can be enhanced. The method includes three steps in accordance with the “ecological sources–ecological corridor–ecological pattern” paradigm [32]. First, ecological sources were recognized by incorporating the supply and demand of ESs. Then, the resistance coefficient was revised using nighttime light intensity data and the ecological risk index, combined with the geological disaster risk index, the soil erosion sensitivity index, and the land desertification risk index. Finally, ecological corridors were selected using the MCR model and some key nodes were recognized according to circuit theory. Figure 2 shows the overall technological framework.

Table 1. Data source and usage.

Data	Usage	Data Source
LULC	Carbon storage, outdoor recreation service, and ESP identification	http://www.resdc.cn/ (accessed on 28 July 2021)
DEM	Geological disaster risk calculation	http://www.gscloud.cn/ (accessed on 10 June 2020)
Slope, aspect, lithology, distance to river, and distance to fault	Geological disaster risk evaluation	Calculated using ArcGIS software
NDVI	Grain production service identification	http://lpdaac.usgs.gov/ (accessed on 28 July 2021)
ET	Water provision service calculation	http://lpdaac.usgs.gov/ (accessed on 28 July 2021)
Annual precipitation data	Water provision service calculation	http://www.geodata.cn/ (accessed on 28 July 2021)
Annual runoff data	Water provision service calculation	www.csdn.store (accessed on 28 July 2021)
Water consumption data	Water provision service calculation	Fujian Bulletin of Water Resource
Population, grain yield, and consumption data	Grain production service identification	http://tj.fujian.gov.cn/ (accessed on 4 August 2021)
Nighttime light data	Ecological resistance coefficient calculation	https://eogdata.mines.edu/nighttime_light/annual/v21/2020/ (accessed on 4 August 2021)
Soil erosion special survey and monitoring data	Soil erosion risk evaluation	Nanjing Center, China Geology Survey

**Figure 2.** Research framework for ESP construction, which includes an assessment of ES supply and demand, ecological source identification, ecological risk evaluation, resistance coefficient revision, and ecological corridor selection.

2.3.1. Identification of Ecological Sources

The first step of ESP construction is to determine ecological sources that refer to key areas contributing to ecological processes, maintaining regional ecological security, and providing ESs [10,11,14]. Regions with high ecological value are usually selected as ecological sources. From the perspective of provisioning ESs to humans, ecological sources should ensure not only a sustainable supply of ESs but also effective human demand [31,33]. As a result, the ecological sources considered in this study are recognized by linking the provision and demand of ESs.

Selection of ESs

Given the special ecological and environmental issues and factors affecting urban agglomeration, high water resource demand and high carbon emissions should not be neglected. Due to the undulating topography, forestland is the dominant land cover

type, and there is a lack of sufficient cropland in the FDU. Therefore, grain supply is important to ecological security. In addition, outdoor recreation services cannot be ignored, as humans need outdoor green space to be close to and experience nature, especially in highly urbanized areas. As a result, four important ESs—carbon storage, water provision, grain production, and outdoor recreation—are selected.

Assessment of ES Supply and Demand

(1) Carbon storage

As an essential regulating function, carbon storage is measured by the quantity of carbon that remains in different pools [34–36]. Carbon density values vary among land use types, and changes in regional land use patterns can lead to ecosystem carbon stock changes in ecosystem carbon storage. Thus, we estimate the carbon density as shown in Table 2, a very important input parameter, in each carbon pool for different land cover types through the InVEST model, using data derived from the China Ecosystem Research Network Data Center (<http://www.nesdc.org.cn/> (accessed on 4 August 2021)), and we also refer to several studies [37–40].

$$S_{cs} = \sum_{i=1}^n A_i \times (C_{above_i} + C_{below_i} + C_{soil_i} + C_{dead_i}) \quad (1)$$

where S_{cs} is the supply of carbon storage services (ton); A_i is the area of the i th type of LULC; C_{above_i} denotes the carbon density of aboveground biomass (t/ha); C_{below_i} denotes the carbon density of belowground biomass (t/ha); C_{soil_i} represents the carbon density of soil (t/ha); C_{dead_i} represents the carbon density of dead matter (t/ha); i denotes the index of LULC; and n represents the number of land use types.

Table 2. Carbon density in various components of different land use types t/ha.

Land Use Type	Above	Below	Soil	Dead
Cultivated land	11.80	0	82.60	2.20
Forest	155.69	60.67	124.80	16.80
Bushwood	6.31	4.84	35.89	3.480
Grassland	1.85	26.87	54.04	3.03
Water	8.43	4.10	0	0
Construction land	0	0	0	0
Unused land	0.36	0.53	21.95	0

Demand for carbon sequestration services is characterized using carbon emissions, which are obtained by multiplying standard coal consumption with a carbon emission rate (Equation (2)). Coal consumption originates from industry, agriculture, the service industry, and household sources. For the purpose of spatial mapping, carbon emissions associated with industry, agriculture, the service industry, and household sources are assigned equally to the grids containing agricultural, industrial, commercial and service, and residential land, respectively. Agricultural land mainly includes cropland and grazed grassland; industrial land includes land for mining and industrial manufacturing; commercial and service land refers to land used for commercial, financial, catering, hotel, and other operating service buildings and their corresponding ancillary facilities; and residential land consists of rural and urban residential land.

$$D_{cs} = (E_I + E_A + E_S + E_h) \times C_t \quad (2)$$

where D_{cs} is the demand for carbon storage services (ton); E_I , E_A , E_S and E_h are the standard coal consumption from industry, agriculture, service industry, and households, respectively (ton); and C_t is the carbon emission rate of coal, which is set to 0.68, according to China's National Development and Reform Commission.

(2) Water provision

Water provision is the service that an ecosystem provides to retain and intercept rainfall within a given region [41]. Water provision in the FDUA is calculated using the water balance equation (Equation (3)).

$$S_w = P - ET - runoff \quad (3)$$

where S_w is the annual water yield (m^3); P represents the annual rainfall amount (mm); ET denotes annual evapotranspiration (mm); and $runoff$ denotes annual runoff (mm).

Water demand can be expressed by actual water consumption in agriculture, industry, households, and ecological processes [42]. The amount of water consumed for agriculture, industry, household, and ecological processes in the FDUA is equally assigned to grids used as agricultural, industrial, residential, and ecological land, respectively. Ecological land mainly includes forestland and natural grassland.

$$D_w = W_A + W_I + W_D + W_E \quad (4)$$

where D_w denotes the water demand (m^3) and W_A , W_I , W_D and W_E are the annual water consumption (m^3) of agriculture, industry, households, and ecological processes, respectively.

(3) Grain production

The grain production function is a significant manifestation of agricultural ESs, and the normalized differential vegetation index (NDVI) extracted from remote sensing data is indicative of potential grain yield [43,44]. According to the linear relationship between crop yield and the NDVI, grain production is rasterized and spatially distributed (Equation (5)). In this study, the grain yield data by district and county are derived from the statistical yearbook officially released online by the Fujian Provincial Bureau of Statistics.

$$S_g = \frac{NDVI_{ij}}{NDVI_i} \times GP_i \quad (5)$$

where S_g is the supply of grain (t/ha); $NDVI_{ij}$ is the j th pixel of the $NDVI$ of the i th county; $NDVI_i$ is the $NDVI$ of the i th county; and GP_i is the grain yield of the i th county (t/ha).

To evaluate the degree of food security, it is necessary to measure the demand for grain. In this study, we mainly focus on the household consumption of grain [45]. Thus, grain demand is estimated using daily consumption by urban and rural residents multiplied by the population density (Equation (6)).

$$D_g = G_u \times pop_u + G_r \times pop_r \quad (6)$$

where D_g is demand for grain (t/ha); G_u and G_r represent annual grain consumed per person residing in urban and rural areas, which are 98.38 (t) and 167.12 (t), respectively; and pop_u and pop_r denote the population density (person/ha) in urban and rural areas, respectively.

(4) Outdoor recreation services

Opportunities for daily outdoor recreation are especially important, as urban dwellers often have limited exposure to natural or seminatural ecosystems [46]. The supply of recreation services is estimated by the degree of naturalness, which is related to the potential of different types of LULC to provide access to nature. LULC types are grouped and ranked from 0 (low) to 10 (high) to evaluate the degree of naturalness according to the intensity of human use and activities [47], as shown in Table 3 [27]. The underlying demand for recreation services is expressed as the fundamental right of all people to enjoy exposure to nature. The local government of Fujian Province recommended including 15.03 m^2 of green space per capita by 2020 [48].

$$S_{or} = \frac{NV_i - NV_{min}}{NV_{max} - NV_{min}} \quad (7)$$

$$D_{or} = G_{avg} \times pop \quad (8)$$

where S_{or} and D_{or} denote the supply and demand of outdoor recreation services, respectively; NV_i is the NV of the i th type of LULC; NV_{max} and NV_{min} are the maximum and minimum NVs, respectively; pop denotes population density; and G_{avg} denotes government guidance on green space.

Table 3. Naturalness values (NVs) of different LULC types.

LULC	NV	LULC	NV	LULC	NV
Built areas	0	Gardens	6	Green urban areas	6
Bare soil	2	Wetlands	6	Cropland	3
Deciduous broadleaf forest	10	Water reservoirs	6	Evergreen broadleaf forest	10
Coniferous forest	8	Artificial water	4	Shrubland/Grassland	8

Ecological Source Identification

In this study, the ecological source should not only guarantee sufficient supply but also satisfy human demand. Thus, ecological sources are identified by linking the actual supply of the ecosystem with the demand of humans. The following indicators are employed to reveal the ES supply–demand balance of a single ES for each pixel.

First, an ecological source should guarantee a sustainable supply of ESs. As shown in Equation (9), after normalizing the supply of the four ESs to remove the dimensionality effect, the mean value for the ecological background is computed.

$$Sup = \frac{1}{n} \sum_{i=1}^n \frac{S_i - S_{i,min}}{S_{i,max} - S_{i,min}} \quad (9)$$

where Sup denotes the average supply of the multiple ESs, S_i is the value of the i th ES supply, $S_{i,max}$ and $S_{i,min}$, respectively, indicate the maximum and minimum values of the corresponding ES; and n denotes the number of ES categories which, in this study, equals 4.

Whether the supply and demand of ESs are spatially well-matched can be measured by an indicator known as the ecological supply–demand ratio (ESDR), which can also indicate an ecosystem’s potential ability to maintain the sustainability of ESs [49,50].

$$ESDR_i = \frac{S_i - D_i}{(S_{i,max} + D_{i,max})/2} \quad (10)$$

where D_i denotes the value of demand for the i th ES, with $D_{i,max}$ set as the corresponding maximum value of human demand. A positive $ESDR_i$ implies a surplus of ESs, whereas a negative value denotes a deficit and a zero value refers to a balanced state.

To assess the supply and demand of various ESs as a whole, the comprehensive ecological supply–demand ratio (CESDR) can be employed as a descriptor of the state of ESs, determined by the arithmetic mean of the ESDR [29].

$$CESDR = \frac{1}{n} \sum_{i=1}^n ESDR_i \quad (11)$$

In this paper, ecological sources with high supply and comprehensive supply–demand ratios of ESs are extracted, which should not only have high supply to maintain ecological function but also a stable state for supply–demand relationships. Specifically, the calculation results of Sup_j and $CESDR$ are first ranked into three levels with the natural breaks classification method, and then patches are extracted from the intersection of regions with level 3 of Sup_j and $CESDR$.

2.3.2. Construction of the Ecological Resistance Surface

The ecological resistance coefficient refers to the cumulative resistance overcome by a species as it moves through a heterogeneous landscape. The traditional method of assigning resistance coefficients considers only the LULC type, assuming that different land-use types are associated with different resistance values for the movement of species and energy. The method for assigning the basic resistance coefficient value based on LULC type is shown in Table 4. However, the potential impact of human activity and regional ecological risk are also related to the resistance coefficient [51].

Table 4. Basic resistance coefficient value (R) assignment.

LULC Type	Forest	Grassland	Cropland	Waterbody	Bare Soil	Built Areas
R	1	10	30	50	300	500

The FDU is exposed to ecological risk, including geological disasters, land desertification, and soil erosion risk. Ecological risk has a certain impact on regional ecological connectivity, which in turn hinders species' migration processes. The FDU is a typical southern red-soil hilly area that is highly susceptible to soil erosion due to frequent and intensive precipitation and heavy granite weathering. Severe soil and wind erosion cause serious losses of clay materials, such as aluminum and iron in the soil, resulting in land desertification. The geological structure of the FDU is complex, with many mountainous areas and steep slopes in some areas, coupled with heavy rainfall during the typhoon season, leading to greater susceptibility to geological hazards, such as landslides, collapses, and mudslides in the region. These geological problems pose great risks to the ecosystem and affect landscape connectivity between patches. In Equation (12), the soil erosion sensitivity index SE_i indicates the magnitude of the soil erosion problems, which is determined according to the intensity of the soil erosion investigation and monitoring results. The sensitivity index values of soil erosion are set as 0.9, 0.7, 0.5, 0.3, and 0.1 based on the corresponding intensity of soil erosion (severe, intense, moderate, light, and slight, respectively). The geological disaster risk index GDR_i is calculated using the "hazard–vulnerability–exposure" three-dimensional evaluation approach, which is represented as $GDR_i = H \times V \times E$, where H , V , and E are the hazard, vulnerability, and exposure of geological disasters, respectively. The details of the method, introduced in [52], are not presented, due to space limitations. Then, disaster risk is classified by the natural break point method into five levels (highest, higher, moderate, lower, and lowest) with values of 0.9, 0.7, 0.5, 0.3, and 0.1, respectively. Land desertification risk index LD_i data were derived from the Department of Natural Resources of Fujian Province. Risk levels are classified into 5 levels (highest, higher, moderate, lower, and lowest) with scores of 0.9, 0.7, 0.5, 0.3, and 0.1, respectively.

Because high ecological risk implies high resistance among species, the ecological risk index is introduced to revise the basic resistance coefficient. In addition, the basic resistance coefficient cannot represent spatial variation within the same LULC type. Many studies have established a strong correlation between nighttime light data and economic activity [53,54]. Nighttime light intensity is characterized by NPP VIIRS nighttime light data. Higher radiation values of the nighttime light data indicate stronger nighttime light intensity. To better embody diversity with respect to the same land use type, NPP VIIRS nighttime light data reflecting the intensity of human activity are adopted to revise the basic ecological resistance.

$$ERI_i = \text{mean}(SE_i, GDR_i, LD_i) \quad (12)$$

$$RR_i = \frac{NL_i}{NL_a} \times R_i \times \frac{ERI_i}{ERI_a} \quad (13)$$

where the ecological risk index ERI_i is assessed with the mean values of the geological disaster risk index GDR_i , the land desertification risk index LD_i , and the soil erosion sensitivity index SE_i ; RR_i and R_i denote the revised and basic resistance coefficient grid i , respectively; NL_i represents the radiance value of nighttime light of grid i ; and NL_a and ERI_a represent the average radiance value of nighttime light and the average ecological risk index of land-use type a corresponding to grid i , respectively.

2.3.3. Identification of Ecological Corridors

As important channels for energy flow and species migration, ecological corridors improve ecological connectivity among ecological sources [55]. The MCR model shows good outcomes for the effective identification of ecological corridors and provides a spatial analysis method for studying and analyzing regional material flows [56]. Ecological corridors are identified through the MCR model using Linkage Mapper software. The formula is as follows:

$$MCR = f \min \sum_{j=n}^{i=m} D_{ij} \times RR_i \quad (14)$$

where MCR denotes the minimum cumulative resistance value; f is a function of the positive correlation representing the positive relation of the least resistance of any point to all sources in space; D_{ij} is the spatial distance between grid i and grid j ; and RR_i is the ecological resistance coefficient of grid i .

3. Results

3.1. Spatial Patterns of Ecological Sources

3.1.1. Supply and Demand of ESs

(1) Supply of ESs

The average value of the carbon storage supply for the study area was 19.75 t/ha, and the maximum value was 32.21 t/ha. Most of the northern, western, and south-central parts of the FDUA consist of coniferous and evergreen broadleaf forests, where carbon storage values are particularly high. The northern, western, and south-central parts of the FDUA have relatively high carbon storage values, mainly due to high forest coverage in these regions, which are dominated by coniferous and evergreen broadleaf forests. In contrast, urban areas show the lowest values of carbon storage supply.

The average, maximum and minimum values of water provision of ESs in the study area were 5.52×10^3 t/ha, 1.60×10^4 t/ha, and 0, respectively. High values of water provision were concentrated in the northern, western, and southwestern parts of the study area, while low values appeared in the northeastern part and southeast coastal zone (see Figure 3). This pattern is attributed to the hydrological characteristics of the FDUA: rainfall rose from northeast to southwest, while surface runoff in the northeastern region was higher than in the western and northwestern regions of the study area.

The total supply of grain production was 9.22×10^5 t. High grain production service values showed an irregular distribution, as these cultivated land areas were scattered in mountain valleys and alluvial plains, due to the rolling and fragmented terrain. In addition, the study area included a larger area of high grain yield in the northern part than in the southern part.

The supply of outdoor recreation ESs, with an average value of 0.26 ha/ha, showed a spatial distribution similar to that of carbon storage: higher values were mainly concentrated in forested mountainous areas, while the urban center showed low outdoor recreation values.

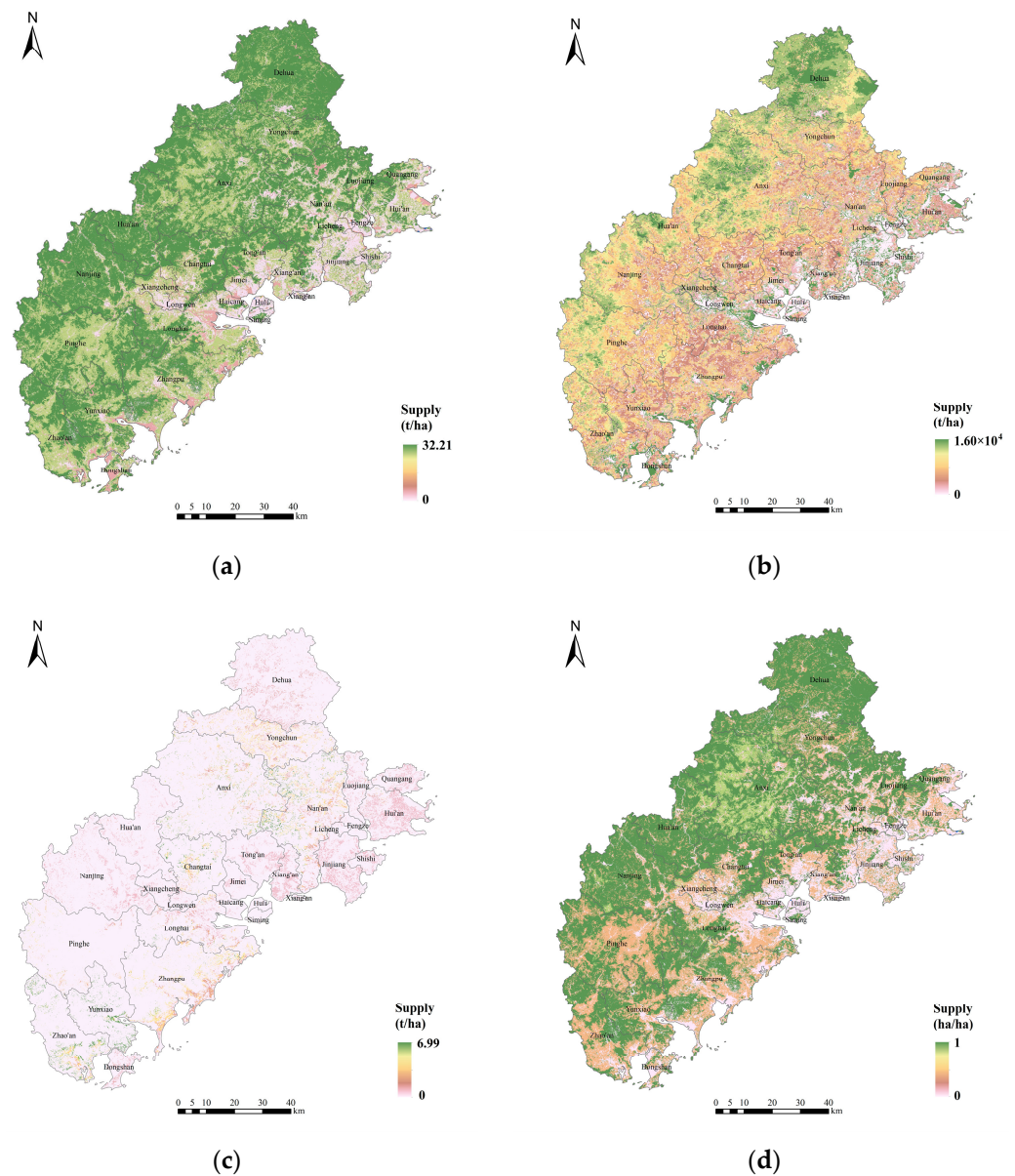


Figure 3. Supply of ESs: (a) carbon storage; (b) water provision; (c) grain production; (d) outdoor recreation.

(2) Demand for ESs

As shown in Figure 4a, overall, there was low demand for carbon storage in most areas, with an average value of 25.93 t/ha. Carbon storage demand was higher and more concentrated in urban areas, due to the larger resident population and relatively intensive human activities.

Total water consumption reached 5.63 billion tons. As shown in Figure 4b, high demand for water was mainly distributed in two kinds of areas: (1) the eastern region of the study area, where there were high levels of urbanization, and (2) spatially scattered patches of cultivated land with irrigated crops that consumed high volumes of water.

The total grain consumption level was 4.64×10^6 t, which means that grain production supply was insufficient and a considerable proportion of grain needed to be imported. The demand for grain production displayed a spatial pattern similar to that of carbon storage, as shown in Figure 4c. High demand primarily occurred in the densely populated northeastern coastal areas as well as inland urban residential areas.

The average value of outdoor recreation service demand was low at 0.11 ha/ha, which means that most areas showed low demand for outdoor services, due to the hilly terrain occupying over 80% of the study area where population density is low. The city center showed the highest outdoor recreation demand levels, but with an irregular distribution, as shown in Figure 4d.

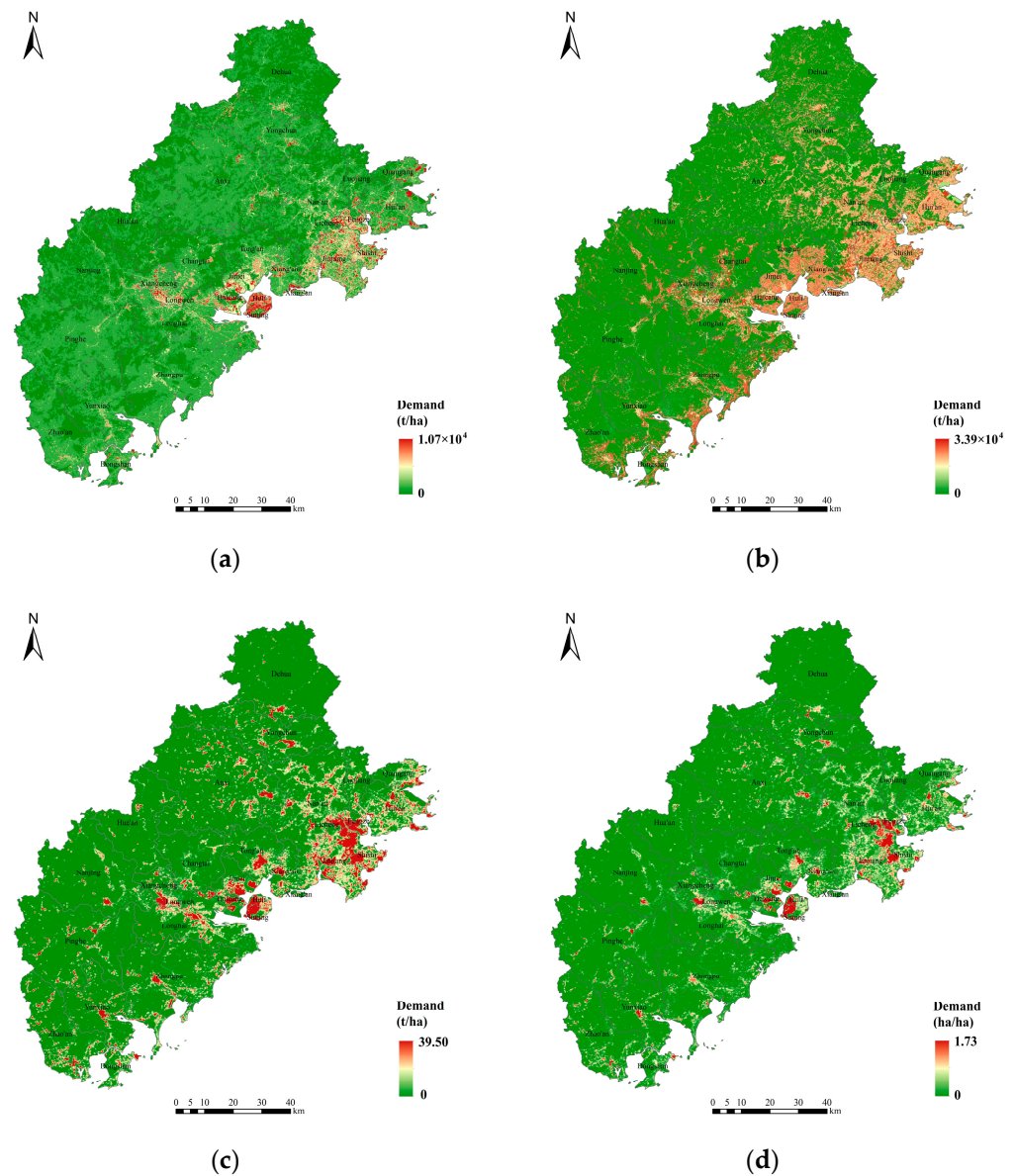


Figure 4. Demand for ESs: (a) carbon storage; (b) water provision; (c) grain production; (d) outdoor recreation.

3.1.2. ES Supply–Demand Ratio Analysis

The ESDR of carbon storage services shows that demand for carbon storage in urban centers exceeded their supply, as shown in Figure 5. Water provision services in most areas were at a surplus, except in eastern coastal areas and middle urban areas of the FDUA, where the ecosystem's water provision failed to cover consumption. The imbalance in grain production supply and demand was more severe than for the other ESs, mainly due to the high demand for grain supply services resulting from the large resident population of the central urban area and surrounding towns. For the ESDR of outdoor recreation services, urban areas suffered from higher demand than supply of outdoor recreation.

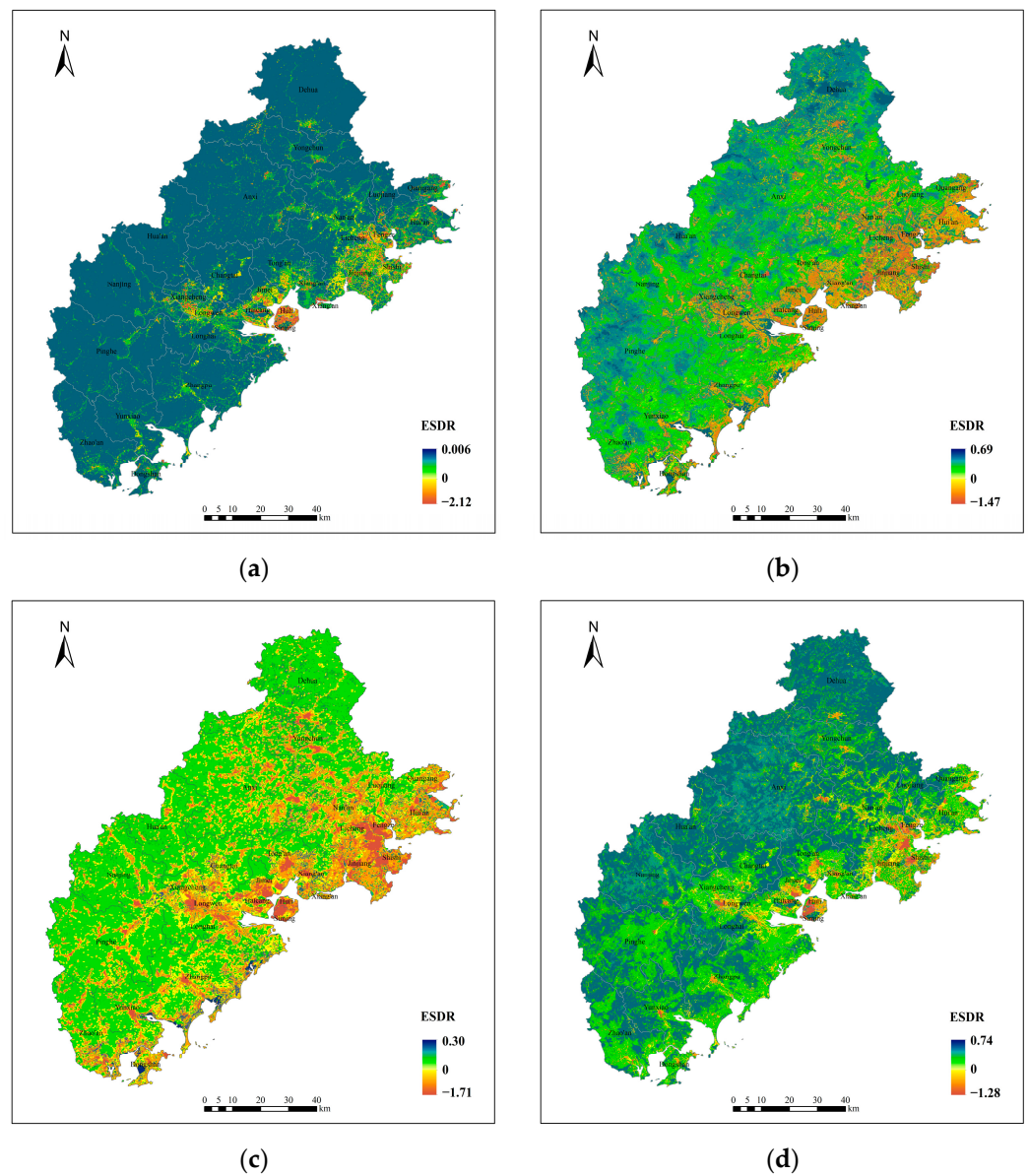


Figure 5. Supply–demand ratio of ESs: (a) carbon storage; (b) water provision; (c) grain production; (d) outdoor recreation.

In general, it was found that in the study area, the supply and demand of ESs were significantly imbalanced. In terms of carbon storage services and outdoor recreation services, regions of high provision were mainly located in forestlands, while high carbon emissions and recreational demand were distributed in densely populated areas. Regarding the water provision services, water supply was significantly higher in the west than in the eastern city centers, because the west is characterized by more rainfall and less evaporation and runoff. In contrast, water consumption is more concentrated in the city center, due to its larger size and higher-density population. Regarding the grain yield services, the spatial distributions of supply and demand were more consistent and well-matched in the mountainous forest area, mainly due to low supply and demand in this region.

3.2. Spatial Distribution of Ecological Sources

Overall, there was a spatial pattern in the supply of ESs, with high values occurring in the west and low values recorded in the east (Figure 6a). The urbanized areas along the coast, such as Quangan, Huai, Fengze, Shishi, and Jinjiang, and the urban areas in the

central part of the FDUA, such as Xiangcheng and Longwen, had a limited supply of ESs, given their large artificial-surface proportions, limited vegetation cover, and weak ecological conditions. The CESDR of ESs presented clear signs of spatial disparity (Figure 6b). High CESDR values were concentrated in the western region with low population density and dense vegetation, resulting from the combination of a high supply and low demand of ESs, which led to a strong capacity to satisfy the ecological requirements of local inhabitants and maintain a sustainable supply of ESs. In the eastern and central regions, where areas of built-up land were large and densely populated, the low CESDR meant the ecosystem supply could hardly meet human ecological demand.

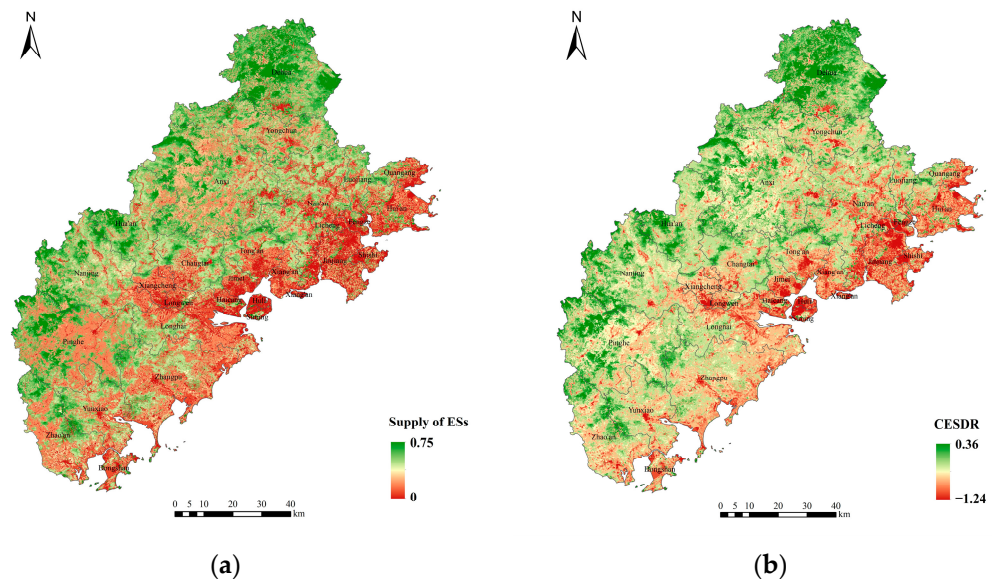


Figure 6. Supply and CESDR of ESs: (a) supply of ESs; (b) CESDR of ESs.

As shown in Figure 6, although the spatial patterns of the two metrics were similar, some differences were found. Especially in Anxi and Pinghe, the supply of ESs was relatively low, but the CESDR was not low, indicating poor ecological conditions in these areas, but sufficient potential to support ecological needs. A coordinated promotion of economic and ecological development should be carried out to improve the quality of ecosystems to meet much of the demand for ecology. Patches in Dehua, Hua'an, and Nanjing showed high supplies and high CESDR levels, implying that the ecological conditions in these areas satisfy ecological demand. Hence, such patches could be recognized as suitable ecological sources.

As shown in Figure 7, the identified ecological sources include 119 patches covering an area of 8359 km², occupying 33.10% of the area of the FDUA. These patches were mostly located in the northern and western hilly and mountainous areas of the region. Some small patches were scattered east of the FDUA and were critical for maintaining the coastal protection function. These ecological sources were mainly composed of forestland, cropland, grassland, and shrubland, among which forestland dominated, accounting for 73.8% of the total ecological source area. There was significant variation in the distribution of ecological sources in different administrative regions, and the distribution was as follows: 53.83% in Quanzhou, 43.26% in Zhangzhou, and 2.91% in Xiamen.

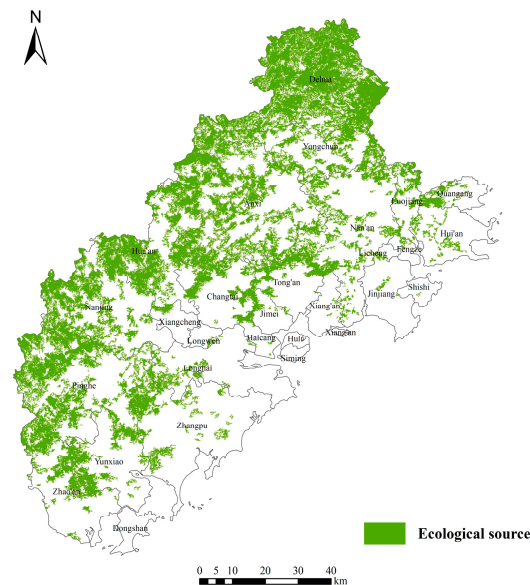


Figure 7. Spatial patterns of ecological sources.

3.3. Spatial Patterns of the Ecological Resistance Surface Coefficient

Ecological risk was used to measure the resistance surface coefficient, which reflects the hindrance to species' migration. The results (Figure 8) show that the geological disaster risk tended to increase from the southern region to the northern inland region. Disaster risk grades by area were ranked as follows: moderate > high > lowest > low > highest, covering 36.02%, 24.11%, 20.04%, 15.79%, and 4.04% of the study area, respectively. The total area with the moderate, high, and highest geological disaster risk levels accounted for 64% of the total area, indicating that the geological hazard risk in the FDUA was generally high. In addition, the sensitivity of soil erosion was generally not high. Most areas were classified as of lowest- and low-sensitivity, accounting for 69.60% of the total area, and the highest-sensitivity areas accounted for 9.71% of the total area. Areas of high and highest sensitivity were scattered in hilly areas covered by red soil. Moreover, a few features resulting from human activities, such as land reclamation on slopes and destroyed vegetation coverage, affected soil erosion during rainfall events. As shown in Figure 8c, overall, the land desertification index values were mostly low. Land desertification risk was higher in the eastern coastal zone, mainly as a result of the marine climate, seawater erosion, and artificial effects of activities such as development and construction. The spatial characteristics of ecological risk are shown in Figure 8d. Regions of high and highest risks were concentrated in the northern region of the study area, including Anxi County and Yongchun County, where altitudes are higher and the population density is lower, and in the eastern coastal areas, including the cities of Shishi, Jinjiang, and Huli District, where land utilization is intensive and ecological conditions are fragile.

The modified resistance surface was derived from the basic ecological resistance surface and the ecological risk, as shown in Figure 9. In comparison with the original values of basic resistance, which ranged from 1 to 500, the spatial diversity of the modified result was more distinct. Among the administrative districts, Huli District had the highest average ecological resistance coefficient value (598.89), followed by Siming District (426.24). Dehua County had the lowest average ecological resistance coefficient value (23.08). Higher ecological resistance coefficients were found mainly around the urban center along the eastern coast. The areas with low ecological resistance coefficients were mainly located in the northern and southwestern areas of the FDUA with high vegetation coverage.

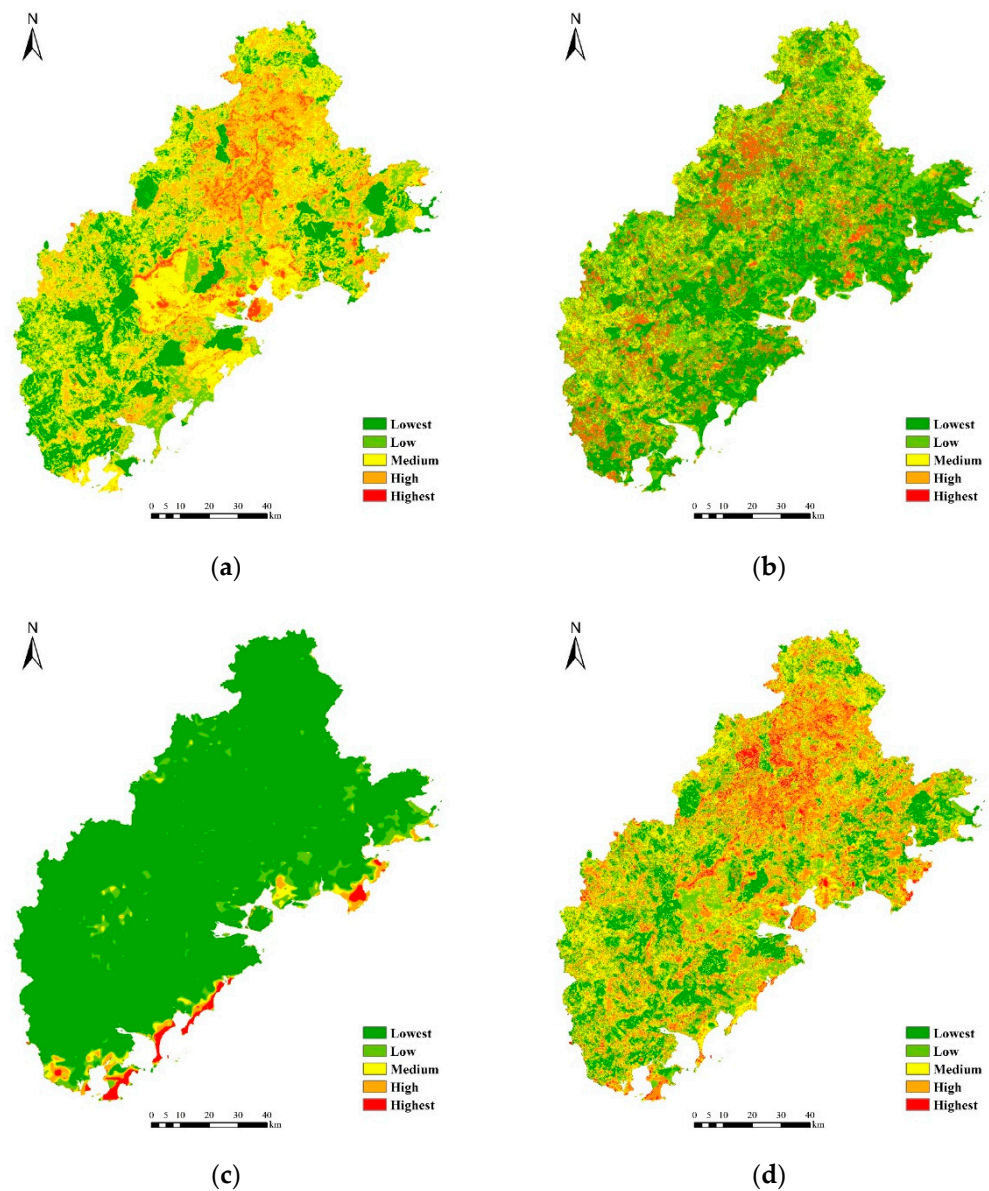


Figure 8. Spatial patterns of ecological risks: (a) geological disaster risk; (b) soil erosion sensitivity; (c) land desertification risk; (d) ecological risk.

3.4. Spatial Distribution of Ecological Corridors

The minimum cost paths between the patches of ecological sources were selected by the MCR model using Linkage Mapper software. As shown in Figure 10, the ESP of the FDUA consisted of ecological sources, with forestland mainly connected by ecological corridors, including 119 ecological source patches, 171 ecological corridors with a total length of 789.04 km, 34 pinch points, 26 barriers, and 48 break points. The ecological corridors were distributed in a web-like shape, effectively linking the ecological patches and providing potential passages for material circulation and energy flow. Ecological corridors had significantly different spatial distributions: ecological sources in the northwest and southwest were large and stretched over long distances, so corridors covered short distances and were few in number; ecological patches in the east were small, fragile, and common, so there were more corridors to connect these patches. Hence, the maintenance of ecological corridors is essential to improving connectivity across the ecological network.

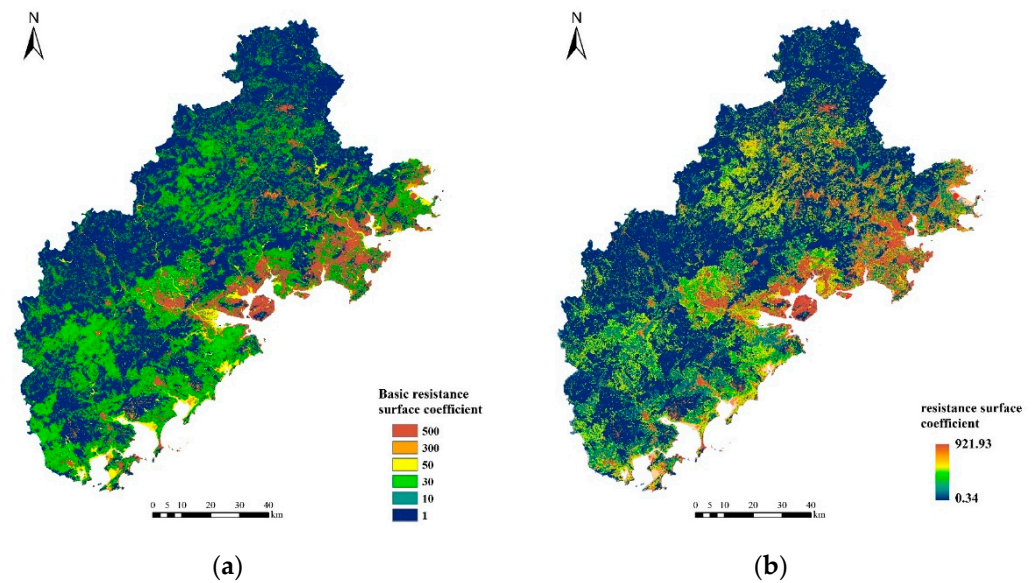


Figure 9. Spatial pattern of the ecological resistance surface coefficient: (a) basic resistance surface; (b) modified resistance surface.

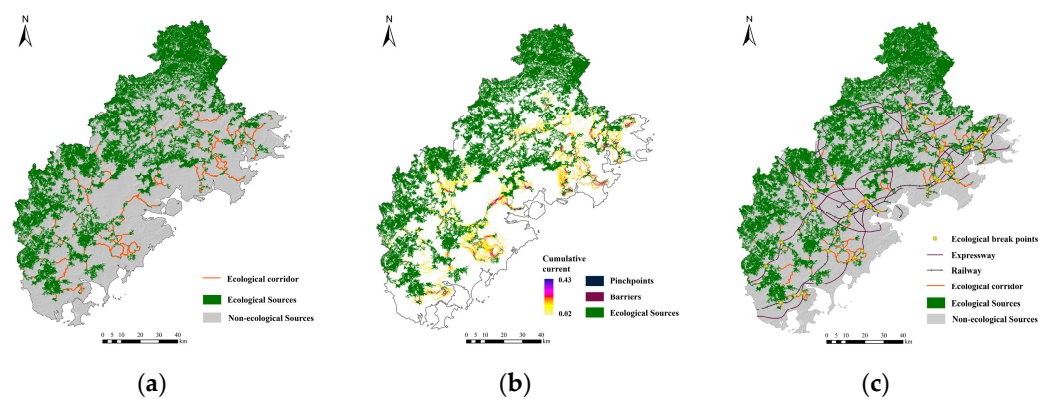


Figure 10. ESPs in the study area: (a) ecological corridor; (b) pinch points and barriers; (c) ecological break points.

The identified pinch points, accounting for an area of 13.82 km², showed a fragmented distribution and spread out in a narrow strip, mainly overlapping with corridors and positioned close to ecological sources. Pinch points were mostly distributed in urban parks, farmland, industrial land, and small pond wetlands in the eastern urban area. This might be a result of the threats of cropland development and urban expansion that hinder connectivity. Barriers were also scattered in the eastern urban area, covering an area of 82.18 km². In terms of LULC types, barriers were mainly located on adjacent industrial lands, at transportation junctions and in residential areas. The ecological corridors in these areas were particularly short and narrow and might be directly cut off with the increase in resistance values at barrier points. As shown in Figure 10c, ecological break points were identified as intersection points between road network and ecological corridors, where the ecological corridor was susceptible to disturbance. Ecological break points appeared more intensive in the northeastern part of the study area. A crisscrossing traffic network divided the landscape into fragmented ecological patches, creating ecological breaks in the continuous corridor network, which was unfavorable to species migration and exchange.

4. Discussion

4.1. Spatial Pattern of ES Supply and Demand Mismatches

We used multiple datasets to evaluate the supply and demand of four essential ESs. The supply of ESs and demand for those ESs are not spatially coupled, and areas with high demand for a particular ES normally have a low supply of the same ES. The findings suggest that water provision and carbon storage services are generally in surplus in the FDUA, but all ESs suffer from a spatial mismatch between supply and demand, particularly in the urban center, due to greater demand. Depending on the assessment results, a spatial analysis of the provision and demand for ESs can quantify how much additional supply of services is required and identify areas where ecological demand should be reduced. Thus, the mismatch between supply and demand for ESs is expected to be mitigated. Furthermore, to achieve this goal, it is unrealistic to only increase the supply of ESs. For instance, the significant disparity between supply and demand for water provision suggests that demand reduction policies are inevitable in urban areas, because reducing consumption or improving water-use efficiency is more promising than substantially increasing water supply to meet ES demand.

4.2. Optimization of Ecological Sources

As expected, the spatial distribution of ecological sources was uneven. Figures 5–7 show that the selected ecological sources are mainly located in the western part of the study area, while ecological demand pressure shows an agglomerated distribution in the eastern and northern parts of the study area. The uneven distribution of ecological sources makes it difficult for ecological services provided by the existing ecological sources to effectively cover high-demand areas. The mismatch between the supply of natural ecological services and the demand for human ecological services will cause a degradation of ecosystem structure and affect ecological function. Therefore, expanding ecological sources is a strategy for balancing the supply and demand of regional ecological services.

4.3. Guidance for the Development of Ecological Policies in the FDUA

After overlaying the identified ecological sources with nature reserves above the province level, the overlapping area between the two accounts for 59.90% of the total area of the reserves, as shown in Figure 11. The coincident part includes the national forest park and nature reserve areas, such as the Daiyunshan nature reserve area and Shiniushan forest park, showing that the ESP is constructed with full consideration of areas critical to protecting the local ecological environment. Moreover, Figure 12 shows that most ecological sources are located within key ecological function areas planned by the government. The identified ecological corridors are spatially close to those planned by the government. Such spatial consistency proves the reliability of the method proposed in this paper. However, it should be noted that the coverage area of these nature reserves is relatively small, and the establishment of protected areas alone is not sufficient to meet ecological demands. In addition, current regional ecological protection policies still focus on the designation of ecological red lines that include forest parks, nature reserves, geological parks, critical scenic areas, wetland parks, world heritage sites, and so on. Ecological security is maintained through a policy of prohibiting land development within the ecological red line boundary to protect habitats of endangered species and ecosystems. Although policy has had some positive effects on the conservation of ecological lands, it does not adequately consider ecosystem structure and function or measure the supply and demand of ecosystems. The effects of ecological protection would be stronger if the delineation of the ecological red line could be integrated into the supply and demand of ecosystems.

5. Conclusions

The study of ESPs, considering ecological supply and demand, is important for protecting regional ecological security and maintaining regional sustainability. Taking the FDUA as an example, this paper identified ESPs based on the MCR model. Ecological sources were characterized by the intersection of patches with high supply and a comprehensive supply–demand ratio of the ESs. The ecological risk index was constructed by combining various factors, such as the soil erosion sensitivity index, the geological disaster risk index, and the land desertification risk index. The ecological risk index was then coupled with the night light index to correct basic ecological resistance. Ecological corridors, pinch points, barriers, and ecological break points were identified through a MCR model and circuit theory.

The supply and demand of ESs showed significant spatial heterogeneity. This was particularly evident from coastal hilly cities to inland mountain cities, where supply showed an increasing gradient, while demand showed the opposite trend. There was a distinct mismatch between the supply and demand of ESs in the study area, which made the spatial distribution of ecological sources uneven to some extent. The corridors connecting ecological sources are distributed along mountains and forest belts. The ESPs in the FDUA consisted of 119 ecological source patches, 171 ecological corridors, 34 pinch points, 26 barriers, and 48 break points. Most of the pinch points, barriers, and break points were concentrated in the eastern region with heavy human disturbance, where ecological protection and restoration should be strengthened to ensure the smooth flow of ecological corridors.

It should be noted that this study has some limitations. First, we assessed four kinds of ESs, due to data limitations. It was difficult to completely identify ESs. Evaluation methods need to be improved to better identify ecological sources, especially for estimating ES demand. Second, the ecological sources were extracted based on spatial characteristics of the supply and demand of ESs. However, determining ways to control the optimal area proportion of ecological sources in the study area still needs to be further studied. Third, regarding ecological corridors, this study identified corridors without considering their width. A corridor's width directly affects its ecological function. Further efforts should be made to determine the width of each corridor involved in a security pattern.

Author Contributions: Conceptualization, X.N.; methodology, X.N.; software, H.N. and Q.M.; validation, X.N., H.N. and Q.M.; formal analysis, H.N.; investigation, X.N. and Q.M.; resources, X.N. and H.N.; data curation, X.N.; writing—original draft preparation, X.N.; writing—review and editing, X.N., H.N., Q.M., S.W. and L.Z.; visualization, X.N.; supervision, H.N. and Q.M.; project administration, X.N.; funding acquisition, X.N. and H.N. All authors have read and agreed to the published version of the manuscript.

Funding: This research was funded by the National Natural Science Foundation of China, grant numbers 41901310 and 41801384; the Geological Survey Project of China, grant number DD20211390; and the National Natural Science Foundation of Shanghai Normal University, grant number SK202155.

Institutional Review Board Statement: Not applicable.

Informed Consent Statement: Not applicable.

Data Availability Statement: This research did not include any data obtained through intervention or interaction with individuals. There was no identifiable private information disclosed. The data used are publicly available and the sources are already clearly indicated in the manuscript.

Conflicts of Interest: The authors declare no conflict of interest. The funders had no role in the design of the study; in the collection, analyses, or interpretation of data; in the writing of the manuscript; or in the decision to publish the results.

References

1. Seto, K.C.; Fragkias, M.; Güneralp, B.; Reilly, M.K. A Meta-Analysis of Global Urban Land Expansion. *PLoS ONE* **2011**, *6*, e23777. [[CrossRef](#)] [[PubMed](#)]
2. Haas, J.; Ban, Y. Urban growth and environmental impacts in Jing-Jin-Ji, the Yangtze, River Delta and the Pearl River Delta—ScienceDirect. *Int. J. Appl. Earth Obs. Geoinf.* **2014**, *30*, 42–55.
3. Peng, L.; Wang, X.-X. What is the relationship between ecosystem services and urbanization? A case study of the mountainous areas in Southwest China. *J. Mt. Sci.* **2019**, *16*, 2867–2881. [[CrossRef](#)]
4. Verburg, R.W.; Osseweijer, F. A framework to estimate biodiversity loss and associated costs due to nitrogen emissions from single power plants. *J. Clean. Prod.* **2019**, *239*, 117953. [[CrossRef](#)]
5. Wang, J.; Lin, Y.; Zhai, T.; He, T.; Qi, Y.; Jin, Z.; Cai, Y. The role of human activity in decreasing ecologically sound land use in China. *Land Degrad. Dev.* **2018**, *29*, 446–460. [[CrossRef](#)]
6. Cerretelli, S.; Poggio, L.; Gimona, A.; Yakob, G.; Boke, S.; Habte, M.; Coull, M.; Peressotti, A.; Black, H. Spatial assessment of land degradation through key ecosystem services: The role of globally available data. *Sci. Total Environ.* **2018**, *628–629*, 539–555. [[CrossRef](#)]
7. Bai, Y.; Ouyang, Z.; Zheng, H.; Li, X.; Zhuang, C.; Jiang, B. Modeling soil conservation, water conservation and their tradeoffs: A case study in Beijing. *J. Environ. Sci.* **2012**, *24*, 419–426. [[CrossRef](#)]
8. Baral, H.; Keenan, R.J.; Sharma, S.K.; Stork, N.E.; Kasel, S. Spatial assessment and mapping of biodiversity and conservation priorities in a heavily modified and fragmented production landscape in north-central Victoria, Australia. *Ecol. Indic.* **2014**, *36*, 552–562. [[CrossRef](#)]
9. Abbaszadeh Tehrani, N.; Mohd Shafri, H.Z.; Salehi, S.; Chanussot, J.; Janalipour, M. Remotely-Sensed Ecosystem Health Assessment (RSEHA) model for assessing the changes of ecosystem health of Lake Urmia Basin. *Int. J. Image Data Fusion* **2022**, *13*, 180–205. [[CrossRef](#)]
10. Peng, J.; Pan, Y.; Liu, Y.; Zhao, H.; Wang, Y. Linking ecological degradation risk to identify ecological security patterns in a rapidly urbanizing landscape. *Habitat Int.* **2018**, *71*, 110–124. [[CrossRef](#)]
11. Li, S.; Xiao, W.; Zhao, Y.; Lv, X. Incorporating ecological risk index in the multi-process MCRE model to optimize the ecological security pattern in a semi-arid area with intensive coal mining: A case study in northern China. *J. Clean. Prod.* **2020**, *247*, 119143. [[CrossRef](#)]
12. Xu, J.; Fan, F.; Liu, Y.; Dong, J.; Chen, J. Construction of Ecological Security Patterns in Nature Reserves Based on Ecosystem Services and Circuit Theory: A Case Study in Wenchuan, China. *Int. J. Environ. Res. Public Health* **2019**, *16*, 3220. [[CrossRef](#)] [[PubMed](#)]
13. Yu, K. Security patterns and surface model in landscape ecological planning. *Landsc. Urban Plan.* **1996**, *36*, 1–17. [[CrossRef](#)]
14. Peng, J.; Yang, Y.; Liu, Y.; Hu, Y.; Du, Y.; Meersmans, J.; Qiu, S. Linking ecosystem services and circuit theory to identify ecological security patterns. *Sci. Total Environ.* **2018**, *644*, 781–790. [[CrossRef](#)] [[PubMed](#)]
15. Dai, L.; Liu, Y.; Luo, X.-L. Integrating the MCR and DOI models to construct an ecological security network for the urban agglomeration around Poyang Lake, China. *Sci. Total Environ.* **2021**, *754*, 141868. [[CrossRef](#)] [[PubMed](#)]
16. Wang, C.; Yu, C.; Chen, T.; Feng, Z.; Hu, Y.; Wu, K. Can the establishment of ecological security patterns improve ecological protection? An example of Nanchang, China. *Sci. Total Environ.* **2020**, *740*, 140051. [[CrossRef](#)]
17. Aminzadeh, B.; Khansefid, M. A case study of urban ecological networks and a sustainable city: Tehran’s metropolitan area. *Urban Ecosyst.* **2010**, *13*, 23–36. [[CrossRef](#)]
18. Kong, F.; Yin, H.; Nakagoshi, N.; Zong, Y. Urban green space network development for biodiversity conservation: Identification based on graph theory and gravity modeling. *Landsc. Urban Plan.* **2010**, *95*, 16–27. [[CrossRef](#)]
19. Wang, Y.; Pan, J. Building ecological security patterns based on ecosystem services value reconstruction in an arid inland basin: A case study in Ganzhou District, NW China. *J. Clean. Prod.* **2019**, *241*, 118337. [[CrossRef](#)]
20. Kang, J.; Zhang, X.; Zhu, X.; Zhang, B. Ecological security pattern: A new idea for balancing regional development and ecological protection. A case study of the Jiaodong Peninsula, China. *Glob. Ecol. Conserv.* **2021**, *26*, e01472. [[CrossRef](#)]
21. Baró, F.; Palomo, I.; Zuilian, G.; Vizcaino, P.; Haase, D.; Gómez-Baggethun, E. Mapping ecosystem service capacity, flow and demand for landscape and urban planning: A case study in the Barcelona metropolitan region. *Land Use Policy* **2016**, *57*, 405–417. [[CrossRef](#)]
22. Feng, X.; Fu, B.; Yang, X.; Lü, Y. Remote sensing of ecosystem services: An opportunity for spatially explicit assessment. *Chin. Geogr. Sci.* **2010**, *20*, 522–535. [[CrossRef](#)]
23. Daily, G.C. *Nature’s Services: Societal Dependence on Natural Ecosystems*; Island Press: Washington, DC, USA, 1997; Volume 1, pp. 75–76.
24. de Araujo Barbosa, C.C.; Atkinson, P.M.; Dearing, J.A. Remote sensing of ecosystem services: A systematic review. *Ecol. Indic.* **2015**, *52*, 430–443. [[CrossRef](#)]
25. Ayanu, Y.Z.; Conrad, C.; Nauss, T.; Wegmann, M.; Koellner, T. Quantifying and Mapping Ecosystem Services Supplies and Demands: A Review of Remote Sensing Applications. *Environ. Sci. Technol.* **2012**, *46*, 8529–8541. [[CrossRef](#)]
26. Baró, F.; Haase, D.; Gómez-Baggethun, E.; Frantzeskaki, N. Mismatches between ecosystem services supply and demand in urban areas: A quantitative assessment in five European cities. *Ecol. Indic.* **2015**, *55*, 146–158. [[CrossRef](#)]

27. González-García, A.; Palomo, I.; González, J.A.; López, C.A.; Montes, C. Quantifying spatial supply-demand mismatches in ecosystem services provides insights for land-use planning. *Land Use Policy* **2020**, *94*, 104493. [CrossRef]
28. Honey-Rosés, J.; Pendleton, L.H. A demand driven research agenda for ecosystem services. *Ecosyst. Serv.* **2013**, *5*, 160–162. [CrossRef]
29. Chen, J.; Jiang, B.; Bai, Y.; Xu, X.; Alatalo, J.M. Quantifying ecosystem services supply and demand shortfalls and mismatches for management optimisation. *Sci. Total Environ.* **2019**, *650*, 1426–1439. [CrossRef]
30. Zhai, T.; Wang, J.; Jin, Z.; Qi, Y.; Fang, Y.; Liu, J. Did improvements of ecosystem services supply-demand imbalance change environmental spatial injustices? *Ecol. Indic.* **2020**, *111*, 106068. [CrossRef]
31. Zhang, L.; Peng, J.; Liu, Y.; Wu, J. Coupling ecosystem services supply and human ecological demand to identify landscape ecological security pattern: A case study in Beijing–Tianjin–Hebei region, China. *Urban Ecosyst.* **2017**, *20*, 701–714. [CrossRef]
32. Liu, X.; Wei, M.; Zeng, J. Simulating Urban Growth Scenarios Based on Ecological Security Pattern: A Case Study in Quanzhou, China. *Int. J. Environ. Res. Public Health* **2020**, *17*, 7282. [CrossRef] [PubMed]
33. Hölting, L.; Jacobs, S.; Felipe-Lucia, M.R.; Maes, J.; Norström, A.V.; Plieninger, T.; Cord, A.F. Measuring ecosystem multifunctionality across scales. *Environ. Res. Lett.* **2019**, *14*, 124083. [CrossRef]
34. Onaindia, M.; Fernández de Manuel, B.; Madariaga, I.; Rodríguez-Loinaz, G. Co-benefits and trade-offs between biodiversity, carbon storage and water flow regulation. *For. Ecol. Manag.* **2013**, *289*, 1–9. [CrossRef]
35. He, C.; Zhang, D.; Huang, Q.; Zhao, Y. Assessing the potential impacts of urban expansion on regional carbon storage by linking the LUSD-urban and InVEST models. *Environ. Model. Softw.* **2016**, *75*, 44–58. [CrossRef]
36. Zhao, M.; He, Z.; Du, J.; Chen, L.; Lin, P.; Fang, S. Assessing the effects of ecological engineering on carbon storage by linking the CA-Markov and InVEST models. *Ecol. Indic.* **2019**, *98*, 29–38. [CrossRef]
37. Li, M.; Wu, J.; Yu, C.; Shi, Y. Estimation and spatial analysis of forest carbon stocks based on remote sensing technology in Wuyi Mountain National Reserve of Fujian province. *J. Nanjing For. Univ.* **2014**, *38*, 6–10.
38. Wang, Y.; Weng, B. Estimate of soil organic carbon density and its stock in Fujian Province. *Fujian J. Agric. Sci.* **2005**, *20*, 42–45.
39. Zheng, D.; Liao, X.; Li, C.; Ye, Q.; Chen, P. Estimation and Dynamic Change Analysis of Forest Carbon Storage in Fujian Province. *Acta Agric. Univ. Jiangxiensis* **2013**, *35*, 112–116.
40. Jia, R.; Tong, C.; Wang, W.; Zeng, C. Organic carbon content and storages in the salt marsh sediments in the Minjiang River estuary. *Wetl. Sci.* **2008**, *6*, 492–499.
41. Wang, L.; Zheng, H.; Wen, Z.; Liu, L.; Robinson, B.E.; Li, R.; Li, C.; Kong, L. Ecosystem service synergies/trade-offs informing the supply-demand match of ecosystem services: Framework and application. *Ecosyst. Serv.* **2019**, *37*, 100939. [CrossRef]
42. Jiang, B.; Bai, Y.; Chen, J.; Alatalo, J.M.; Xu, X.; Liu, G.; Wang, Q. Land management to reconcile ecosystem services supply and demand mismatches—A case study in Shanghai municipality, China. *Land Degrad. Dev.* **2020**, *31*, 2684–2699. [CrossRef]
43. Chen, T.; Feng, Z.; Zhao, H.; Wu, K. Identification of ecosystem service bundles and driving factors in Beijing and its surrounding areas. *Sci. Total Environ.* **2020**, *711*, 134687. [CrossRef] [PubMed]
44. Guo, R.; Wu, T.; Liu, M.; Huang, M.; Stendardo, L.; Zhang, Y. The Construction and Optimization of Ecological Security Pattern in the Harbin-Changchun Urban Agglomeration, China. *Int. J. Environ. Res. Public Health* **2019**, *16*, 1190. [CrossRef]
45. Luo, H.; Pan, L.; Yu, Z. Evaluation of grain supply and demand pattern in major grain-producing areas in China based on contribution rate to food security. *Acta Agric. Zhejiangensis* **2020**, *32*, 2077–2087.
46. Plieninger, T.; Bieling, C.; Fagerholm, N.; Byg, A.; Hartel, T.; Hurley, P.; López-Santiago, C.A.; Nagabhatla, N.; Oteros-Rozas, E.; Raymond, C.M.; et al. The role of cultural ecosystem services in landscape management and planning. *Curr. Opin. Environ. Sustain.* **2015**, *14*, 28–33. [CrossRef]
47. Schneiders, A.; Van Daele, T.; Van Landuyt, W.; Van Reeth, W. Biodiversity and ecosystem services: Complementary approaches for ecosystem management? *Ecol. Indic.* **2012**, *21*, 123–133. [CrossRef]
48. 14th Five-Year Plan for Urban and Rural Infrastructure Construction of Fujian Province. Available online: https://www.fujian.gov.cn/zwgk/zxwj/szfbgtwj/202110/t20211013_5704130.htm (accessed on 4 August 2021).
49. Li, J.; Jiang, H.; Bai, Y.; Alatalo, J.M.; Li, X.; Jiang, H.; Liu, G.; Xu, J. Indicators for spatial-temporal comparisons of ecosystem service status between regions: A case study of the Taihu River Basin, China. *Ecol. Indic.* **2016**, *60*, 1008–1016. [CrossRef]
50. Jiang, H.; Peng, J.; Dong, J.; Zhang, Z.; Xu, Z.; Meersmans, J. Linking ecological background and demand to identify ecological security patterns across the Guangdong-Hong Kong-Macao Greater Bay Area in China. *Landsc. Ecol.* **2021**, *36*, 2135–2150. [CrossRef]
51. Pickett, S.T.A.; Cadenasso, M.L.; Rosi-Marshall, E.J.; Belt, K.T.; Groffman, P.M.; Grove, J.M.; Irwin, E.G.; Kaushal, S.S.; LaDeau, S.L.; Nilon, C.H.; et al. Dynamic heterogeneity: A framework to promote ecological integration and hypothesis generation in urban systems. *Urban Ecosyst.* **2017**, *20*, 1–14. [CrossRef]
52. Lin, J.; Lin, M.; Chen, W.; Zhang, A.; Qi, X.; Hou, H. Ecological risks of geological disasters and the patterns of the urban agglomeration in the Fujian Delta region. *Ecol. Indic.* **2021**, *125*, 107475. [CrossRef]
53. Elvidge, C.D.; Sutton, P.C.; Ghosh, T.; Tuttle, B.T.; Baugh, K.E.; Bhaduri, B.; Bright, E. A global poverty map derived from satellite data. *Comput. Geosci.* **2009**, *35*, 1652–1660. [CrossRef]
54. Zhang, Q.; Seto, K.C. Mapping urbanization dynamics at regional and global scales using multi-temporal DMSP/OLS nighttime light data. *Remote Sens. Environ.* **2011**, *115*, 2320–2329. [CrossRef]

55. Zhang, Y.-Z.; Jiang, Z.-Y.; Li, Y.-Y.; Yang, Z.-G.; Wang, X.-H.; Li, X.-B. Construction and Optimization of an Urban Ecological Security Pattern Based on Habitat Quality Assessment and the Minimum Cumulative Resistance Model in Shenzhen City, China. *Forests* **2021**, *12*, 847. [[CrossRef](#)]
56. Zhu, K.-W.; Chen, Y.-C.; Zhang, S.; Yang, Z.-M.; Huang, L.; Lei, B.; Li, L.; Zhou, Z.-B.; Xiong, H.-L.; Li, X.-X. Identification and prevention of agricultural non-point source pollution risk based on the minimum cumulative resistance model. *Glob. Ecol. Conserv.* **2020**, *23*, e01149. [[CrossRef](#)]

Disclaimer/Publisher's Note: The statements, opinions and data contained in all publications are solely those of the individual author(s) and contributor(s) and not of MDPI and/or the editor(s). MDPI and/or the editor(s) disclaim responsibility for any injury to people or property resulting from any ideas, methods, instructions or products referred to in the content.